



Simulation of double buffer layer on CIGS solar cell with SCAPS software

Jingjing Qu¹ · Linrui Zhang¹ · Hao Wang¹ · Xuemei Song¹ · Yongzhe Zhang¹ · Hui Yan¹

Received: 26 March 2019 / Accepted: 31 October 2019 / Published online: 13 November 2019
© Springer Science+Business Media, LLC, part of Springer Nature 2019

Abstract

In a CIGS thin film solar cell, the buffer layer is interposed between the absorber layer and the window layer, which plays an important role in interface electricity. CdS is often used as a buffer layer in CIGS cells. Beside the toxicity of Cd, the main drawback of CdS is its relatively narrow band gap (2.4 eV), which can lead to the current loss due to parasitic absorption. In order to reduce the use of CdS, we try other buffer layers instead of CdS and optimize buffer layer structure. Numerical simulation has been used to explore the effect of different buffer layer materials (CdS and ZnSe) on the performance of CuInGaSe₂ solar cells with SCAPS-1D software. The main photovoltaic parameters of the analog device: open circuit voltage, short circuit current density, fill factor and conversion efficiency (η) were compared and analyzed. The results show that different buffer materials and thickness have great influence on the performance of the cell. In this simulation, CdS buffer layer was replaced by ZnSe material, which has a wider band gap. However, the efficiency of this kind of cell is lower than that of CIGS device with CdS buffer layer because of the bad energy band alignment. In order to improve the short-wave absorption and the efficiency of CIGS cell, we simulated a novel CdS/ZnSe double buffer layer structure. The efficiency of the optimized cell with double buffer layer increases from 18.47% (conventional cell with the same CdS buffer layer thickness) to 19.01%.

Keywords CIGS · Buffer layer · SCAPS

1 Introduction

The CIGS solar cell with tetragonal chalcopyrite structure is currently one of the most promising solar cells, and the highest conversion efficiency has reached 23%. The band gap of CIGS can be adjusted by replacing indium with gallium, so that the solar spectrum can

This article is part of the Topical Collection on Optics in Materials, Energy and Related Technologies 2018.

Guest Edited by Yen-Hsun Su, Songnan Qu, Yiting Yu, Wei Zhang.

✉ Hui Yan
hyan@bjut.edu.cn; yzzhang@bjut.edu.cn; 479640028@qq.com

¹ The College of Materials Science and Engineering, Beijing University of Technology, Beijing 100124, China

be better matched. Because the CIGS material can be deposited on the rigid and flexible substrates by applying various deposition techniques, which expands its applications on the ground. In addition, due to their high radiation tolerance, CIGS solar cell can also be used for space applications (Reinhard et al. 2015; Rampino et al. 2012; Guillemoles 2002; Fischer et al. 2014; Kapur et al. 2008; Nakada 2012; Ramanathan et al. 2003; Romeo et al. 2004). Buffer layer is a very important layer in cell structure and it has many meaningful functions:

1. CIGS solar cell often prepared in the “substrate/Mo/CIGS/buffer layer/i-ZnO/TCO” structure, in which the buffer layer between the absorber layer and the window layer can avoid the reaction between the two and improve the efficiency (Khoshsirat and Yunus 2013).
2. Moreover, the buffer layer can protect the absorber layer from damage by high-energy ions when sputtering the window layer.
3. Since buffer layer is usually highly-resistive, it serves as intermediate layer that can prevent shunting between the TCO layer and the absorber layer.
4. It has a suitable guide band alignment with the absorber layer CIGS and the undoped ZnO layer. Buffer layers affect the band offsets and also the electric field in the junction, and thus the current transport (Pudov 2005).
5. And it has a beneficial interface defect chemistry. It has been reported that the positive charge Cd may form a stable donor defect on the copper deficient chalcopyrite surface, which can produce a suitable charge density and a clear Fermi level position (Wada 1998).

CdS is often used as a buffer layer in CIGS cells. The main drawback of CdS is the relatively narrow band gap, which often leads to the current loss due to parasitic absorption. In addition, the toxicity of Cd is also a serious problem. Therefore, the extensive research on alternative buffer layers is in progress, such as wide-band materials (Zinc oxides, sulphides, and selenides). Among them, ZnSe is one of the most promising materials that can replace CdS at present. ZnSe material is n-type semiconductor so that it can form a p–n junction with the absorber layer. In addition, the bandgap of ZnSe is greater than that of CdS, which make more photons enter into the absorber. However, wide-band gap material will also cause some interface electrical issues.

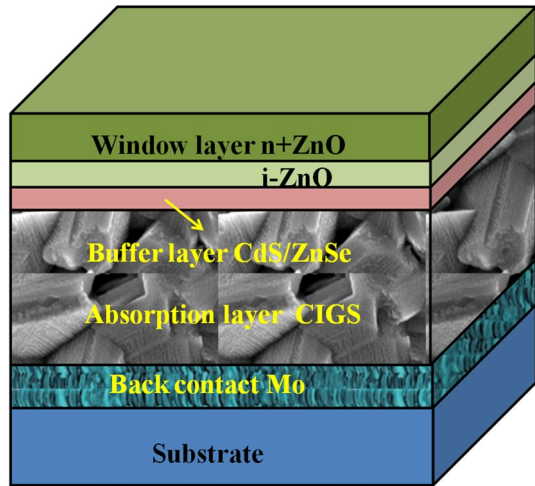
In this paper, SCAPS software is used to simulate the device performance of CIGS solar cell with CdS, ZnSe and double buffer layers (CdS/ZnSe). Under the standard conditions (AM1.5 G, 100 mW/cm², 300 K), the photovoltaic parameters open circuit voltage V_{oc} , short circuit current J_{sc} , filling factor FF, efficiency η of different buffer layers under varied thicknesses are measured. In order to optimize the interface electricity and light absorption, we put forward the double buffer layer for further enhancement.

2 Device structure, simulation method and material parameters

2.1 Cell structure

The basic structure of the CIGS cell used in this simulation is shown in Fig. 1. A layer of Mo is used as the back electrode on the substrate by sputtering. The buffer layer materials

Fig. 1 Schematic structure of a CIGS solar cell



are CdS and ZnSe respectively and $i\text{-ZnO}/n^+\text{-ZnO}$ are used as the window layer. The film layer setting and light entering direction of the simulated cell are as shown in Fig. 2.

2.2 Simulation fitting method

SCAPS is a one dimensional solar cell simulation program developed at the department of Electronics and Information Systems (ELIS) of the University of Gent, Belgium. The software have the ability in solving the basic semiconductor equations, the Poisson equation

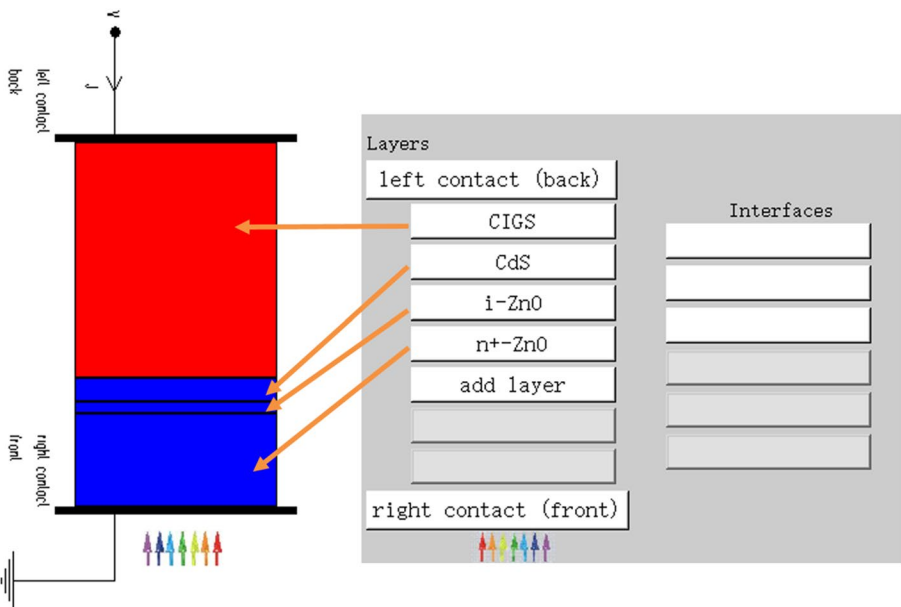


Fig. 2 Simulated cell layer setting and light entering direction

and the continuity equations for electrons and holes (Mostefaoui et al. 2015; Movla 2014). Its operating principle is to find solutions to these equations.

The equations are as follows:

$$\frac{d^2}{dx^2}\psi(x) = \frac{e}{\epsilon_0\epsilon_r}(p(x) - n(x) + N_D - N_A + \rho_p - \rho_n) \quad (1)$$

where ψ is electrostatic potential, ϵ_0 and ϵ_r are relative and the vacuum permittivity, e is electrical charge, p and n are hole and electron concentrations, N_D and N_A are charged impurities of donor and acceptor type, ρ_p and ρ_n are holes and electrons distribution, respectively.

$$\frac{dJ_n}{dx} = G - R \quad (2)$$

$$\frac{dJ_p}{dx} = G - R \quad (3)$$

where J_n and J_p are electron and hole current densities, G is the generation rate. And R is the recombination rate.

Together with appropriate boundary conditions at the interfaces and contacts, this results in a system of coupled differential equations. SCAPS numerically calculates a steady state and a small signal solution of this system. Hereto, the structure is first discretized (creating a mesh). A steady state workingpoint situation is calculated and when required a small signal analysis is performed.

The meshing algorithm of SCAPS provides:

1. Coarse meshing in the middle of a layer.
2. Finer meshing near the interfaces and contacts.
3. Two discretization points (with identical spatial coordinate) for each interface.
4. The mesh can be optimized during calculation.

The first step in every calculation is to discretize the structure. The basic algorithm is designed to provide a lot of points in regions where properties experience large variations (close to interfaces/contacts) and fewer points where the properties are expected to remain fairly constant (in the bulk). Meanwhile, when performing simulations with strong gradings, with multivalent defects or with the IPV-effect, it is possible to optimize the mesh at every iteration step.

2.3 Material parameters

In order to run numerical simulation calculations, the baseline parameters of the solar cell have to be defined to be used as inputs for SCAPS software. The Table 1 shows the basic parameters used for this simulation (Mostefaoui et al. 2015; Oyedele and Aka 2017). The thickness of CIGS is 3 μm , at the same time, we varied the thickness of the varied buffer layers from 0.02 to 0.1 μm and then we simulated the CdS/ZnSe double buffer layer to further enhance cell efficiency. When performing simulations under illumination, SCAPS can specify the illumination conditions. The basis settings are: dark or light, choice of the illuminated side, choice of the spectrum. If users have an optical simulator at their disposal

Table 1 The basic parameters used for this simulation

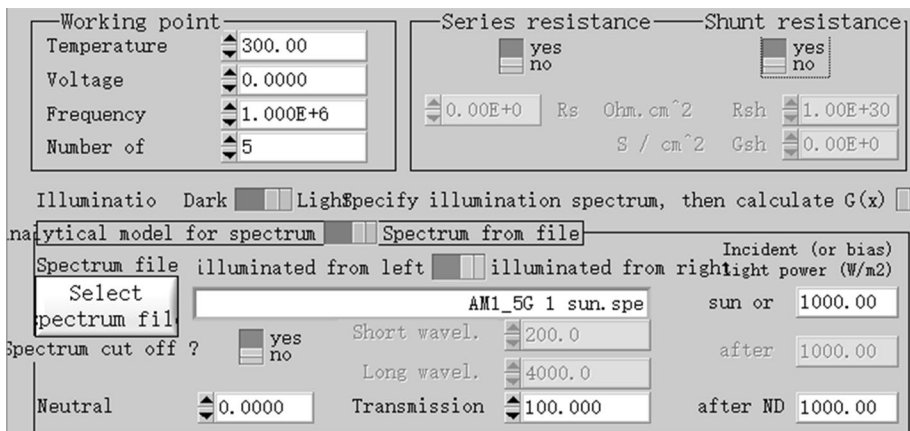
| Parameter | CIGS | CdS | ZnSe | i-ZnO | n ⁺ -ZnO |
|--|------------------------|------------------------|------------------------|------------------------|------------------------|
| Thickness, w (μm) | 3 | Varied | Varied | 0.05 | 0.4 |
| Band gap, E _g (eV) | 1.2 | 2.4 | 2.9 | 3.3 | 3.2 |
| Electron affinity, χ (eV) | 4.0 | 4.2 | 4.2 | 4.4 | 4.4 |
| Dielectric constant, ε/ε ₀ | 13.6 | 10 | 10 | 9 | 9 |
| Density of states at conduction band, N _C (cm ⁻³) | 2 × 10 ¹⁷ | 2 × 10 ¹⁸ | 2 × 10 ¹⁸ | 3.1 × 10 ¹⁸ | 3.1 × 10 ¹⁸ |
| Density of states at valance band, N _V (cm ⁻³) | 1.5 × 10 ¹⁹ | 1.8 × 10 ¹⁹ | 1.8 × 10 ¹⁹ | 1.8 × 10 ¹⁹ | 1.7 × 10 ¹⁹ |
| Electron thermal velocity, δ _e (cm/s) | 1 × 10 ⁷ | 1 × 10 ⁷ | 1 × 10 ⁷ | 1 × 10 ⁷ | 1 × 10 ⁷ |
| Hole thermal velocity, δ _h (cm/s) | 1 × 10 ⁷ | 1 × 10 ⁷ | 1 × 10 ⁷ | 1 × 10 ⁷ | 1 × 10 ⁷ |
| Donor density, N _D (cm ⁻³) | 0 | 1 × 10 ¹⁷ | 5.5 × 10 ⁷ | 1 × 10 ¹⁸ | 1 × 10 ¹⁹ |
| Acceptor density, N _A (cm ⁻³) | 2 × 10 ¹⁶ | 0 | 0 | 0 | 0 |
| Electron mobility, μ _e (cm ² /Vs) | 100 | 70 | 70 | 100 | 100 |
| Hole mobility, μ _h (cm ² /Vs) | 25 | 3 | 3 | 31 | 31 |
| Gaussian defect density, N _t (cm ⁻³) | 1 × 10 ¹⁵ | 1 × 10 ¹⁸ | 1 × 10 ¹⁸ | 1 × 10 ¹⁴ | 1 × 10 ¹⁴ |

they can immediately load a generation profile as well in stead of using a spectrum. Therefore, the structure has been studied under the standard conditions (AM1.5 G, 100 mW/cm², 300 K), as shown in Fig. 3.

3 Simulation results and discussion

3.1 Modeling of various thickness of different buffer layers

The CIGS based solar cells with different buffer layers under AM 1.5 standard condition were simulated. We varied thickness of buffer layers from 0.02 to 0.1 μm while keeping the other

**Fig. 3** Lighting conditions and temperature settings

parameters unchanged to check the effect of thickness on the performance of the CIGS solar cells.

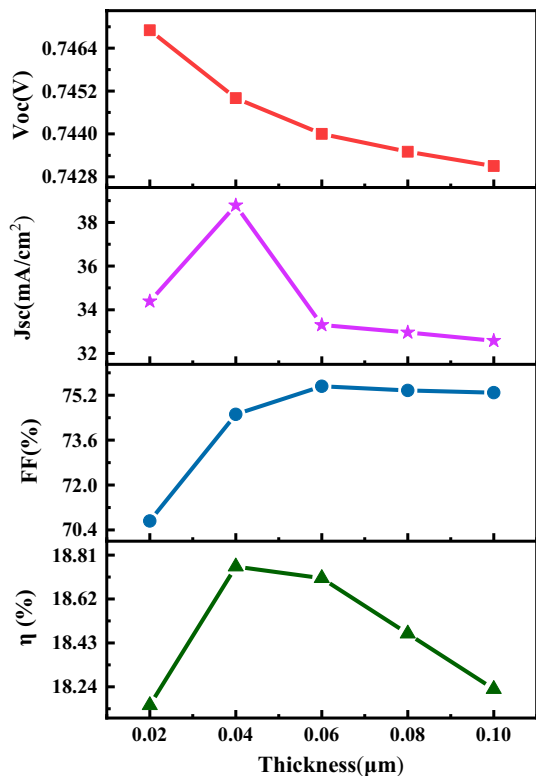
3.1.1 Effect of various thickness of CdS buffer layers

Figure 4 shows the effect of varied thickness (from 0.02 to 0.1 μm) of CdS buffer layer on the main photovoltaic parameters V_{oc} , J_{sc} , FF and η of CIGS solar cell. With the increase of the thickness of the CdS buffer layer, the V_{oc} of the cell gradually decreases, from 0.7469 to 0.7431 eV, a total decrease of 0.51%. J_{sc} first increases and then decreases with the increase of thickness. And the difference between the maximum and the minimum is 16%. FF is growing. And the overall growth is 6%. At last η increases to 18.76% and then decreases to 18.23%, thus reducing 3%. The appropriate buffer layer means the higher electron concentration, which can expand the depleted region of CIGS, then enhance J_{sc} . However, the decrease of the V_{oc} and J_{sc} is due to the parasitic absorption caused by increased thickness of CdS buffer layer, which reduce the generation of photogenerated carriers and the shift of Fermi level of the CIGS absorption layer (Zhang et al. 2018).

From the definition formula of filling factor (4) and efficiency (5), we can see the increase of filling factor and decrease of efficiency are mainly due to the obvious decrease of J_{sc} and V_{oc} when the thickness of CdS reaches 0.04 μm .

$$FF = J_m V_m / J_{sc} V_{oc} \tag{4}$$

Fig. 4 Effect of various thickness of CdS buffer layer



$$\eta = J_m V_m / A_t P_{in} \quad (5)$$

J_m and V_m are currents and voltages at maximum output power respectively. The total area of solar cells and the power of incident light per unit area are A_t and P_{in} , respectively.

In general, for CdS, a thin buffer layer should be used to make the cell achieve the best overall results.

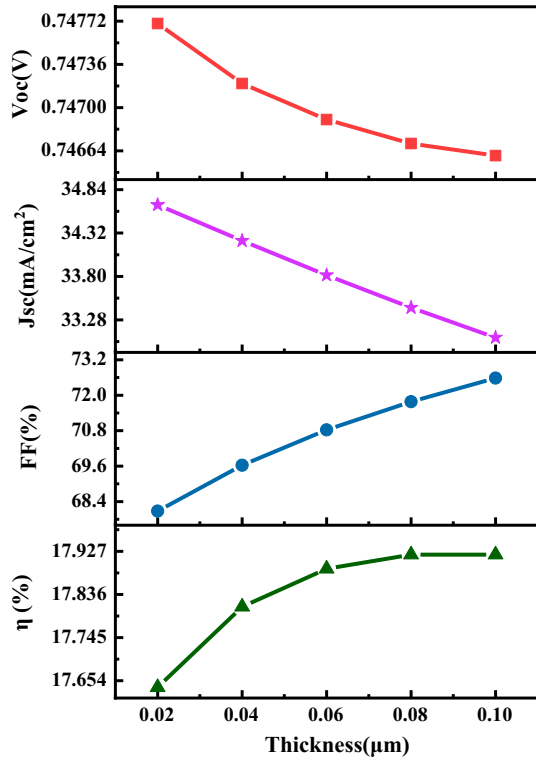
3.1.2 Effect of various thickness of ZnSe buffer layers

Figure 5 exhibits the effect of different thickness of ZnSe buffer layer on the main photovoltaic parameters V_{oc} , J_{sc} , FF and η of CIGS solar cell. The thickness of the ZnSe layer varies from 0.02 to 0.1 μm . The change of V_{oc} is similar to that of CdS. V_{oc} decreases with the increase of buffer layer thickness, but the value changes little, only decreases by 0.15%. Because ZnSe has a larger band gap and lower carrier concentration, which has little effect on the depletion region. And J_{sc} decreases with the increase of buffer layer thickness. From 34.66 to 33.07 mA/cm^2 , the J_{sc} declines by 5%. FF increases from 68.08 to 72.58% and increases by 7%. As the thickness of the buffer layer increases from 0.02 to 0.1 μm , η also increases gradually, from 17.64 to 17.92%, which increases 2% overall.

3.1.3 Effect of various thickness of buffer layers on QE curve

The thickness of buffer layer will directly affect the absorption of photons. Therefore, QE of the CIGS solar cell with different buffer layers were presented in Fig. 6. The response

Fig. 5 Effect of various thickness of ZnSe buffer layer



intensity of short wave band decreases with the increase of CdS buffer layer thickness, as shown in Fig. 6a. Figure 6b depicts the QE curve of solar cell with ZnSe buffer layer. It can be obtained that the long band response of the cell is significantly affected by the variation of ZnSe buffer thickness. The thinner buffer layer the better the long band response.

3.1.4 Effect of various thickness of buffer layers on recombination curve

Figure 7 shows the total recombination curves of CIGS cells with the 20 nm and 40 nm CdS buffer layers. When the thickness of CdS layer is 40 nm, the solar cell has the highest efficiency. When the thickness of CdS layer is 20 nm, the efficiency of the cell is the lowest. In fact, there is little difference in the recombination rate between them in the whole absorption layer (See Fig. 7a). However, it can be seen that the carrier recombination rate of cell with 40 nm CdS layer is the lower than that with 20 nm at buffer layer, as shown in Fig. 7b. The reduction of the recombination can improve the FF.

Fig. 6 The QE curve of CdS/ZnSe (a/b) buffer layer with various thickness

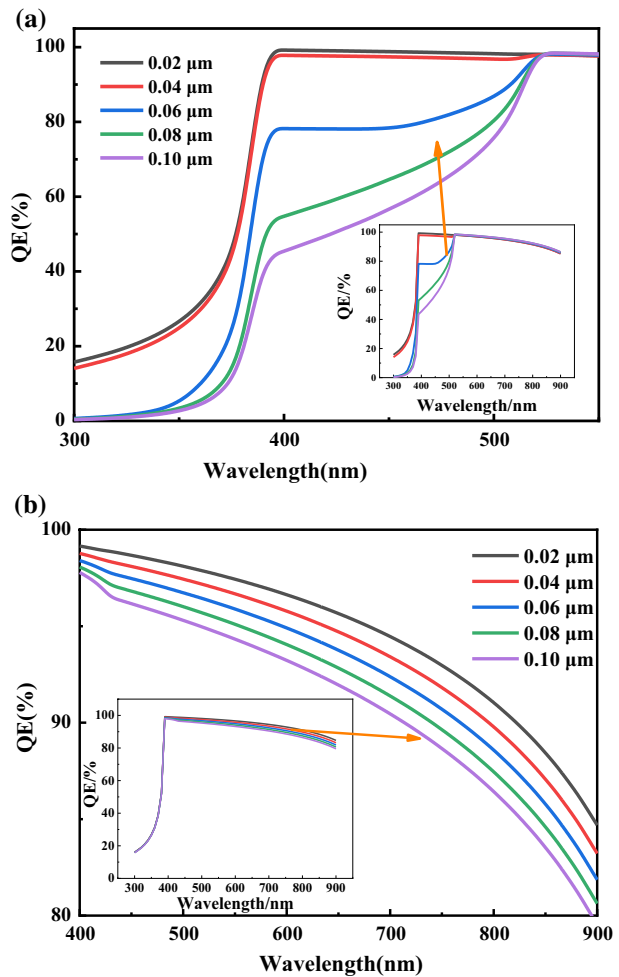


Fig. 7 The recombination curve of CIGS cells with CdS buffer layers (various thickness) (a) and the local enlargements of curve (b)

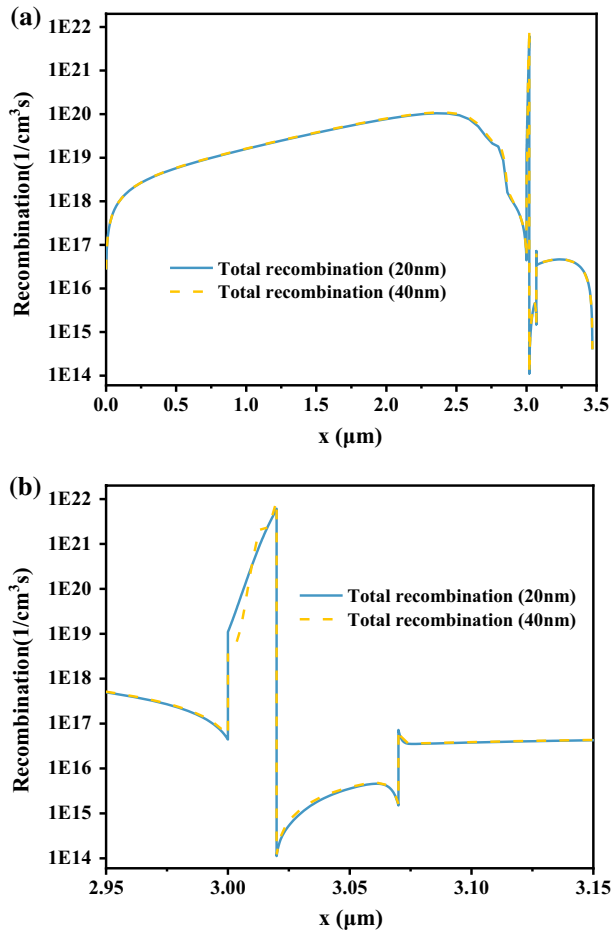
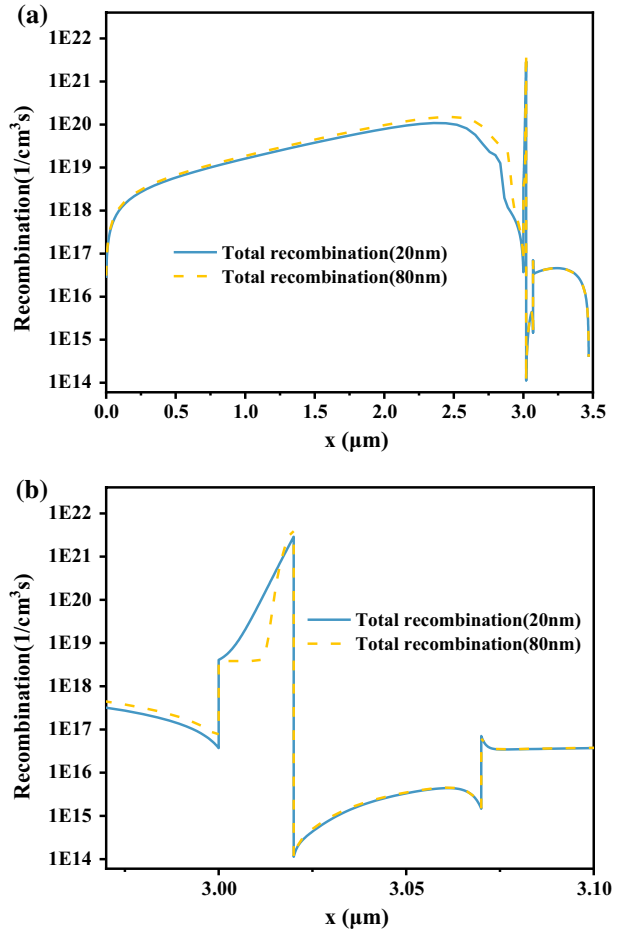


Figure 8 shows the recombination curves of CIGS cells with 20 nm (the lowest η) and 80 nm (the highest η) ZnSe buffer layers. Interestingly, the carrier recombination rate intensifies as the thickness of the ZnSe layer increases, where is located within the CIGS layer and closer to the interface of the ZnSe layer (see Fig. 8a). The increase of recombination rate in absorption layer can be attributed to increase of conduction band edge, which block the electron separation. But from Fig. 8b), in the ZnSe layer, the recombination rate of the device with 80 nm buffer layer is much lower than that of the cell with 20 nm buffer layer. And the improved η is mainly attributed to the increase of FF.

It can be seen from the previous studies that when CdS and ZnSe are selected as buffer layers of solar cells, their effects on V_{oc} , J_{sc} , FF and η are different. When ZnSe is used as buffer layer, the blue correspond of the cell can be improved, thus the short circuit current of the cell can be increased. At the same time, it will also increase of the recombination rate of the absorption layer. But CdS has the appropriate band alignment. Therefore, in order to further improve the performance of solar cells, we intend to obtain the advantages of two buffer layers by simulating a double buffer layer.

Fig. 8 The recombination curve of CIGS cells with ZnSe buffer layers (various thickness) (a) and the local enlargements of curve (b)



3.2 Modeling of double buffer layers

Figure 9 shows the photovoltaic parameters for the CIGS with CdS, ZnSe and CdS/ZnSe buffer layers. All the thickness of buffer layers are the same (80 nm), and CdS/ZnSe buffer layer consists of 30 nm CdS and 50 nm ZnSe. The conversion efficiency (CdS and ZnSe) of the simulated CIGS cell is close to the experimental result obtained from the real device [21.7% (Jackson et al. 2015), 14.4% (Varshni 1967)]. The higher Voc of the cell with ZnSe buffer layer can be attributed to the enlarged band gap. It can be observed that Jsc and FF with ZnSe/CdS double buffer layer are better than the CIGS solar cell with only ZnSe layer and the same as that of the CIGS solar cell with conventional CdS layer. Meanwhile, the Voc of the device with double buffer layer is better than that with CdS buffer layer, which makes the efficiency of conventional device increases from 18.47 to 19.01%.

Figure 10 shows QE of the CIGS solar cell with CdS, ZnSe and CdS/ZnSe buffer layers. As can be seen from the Figure, the response intensity of the solar cell with ZnSe and CdS/ZnSe double buffer layer are stronger than that with CdS in the short wave band from 300 to 380 nm, which makes their Jsc higher than that with CdS. In the wave band from 450 to

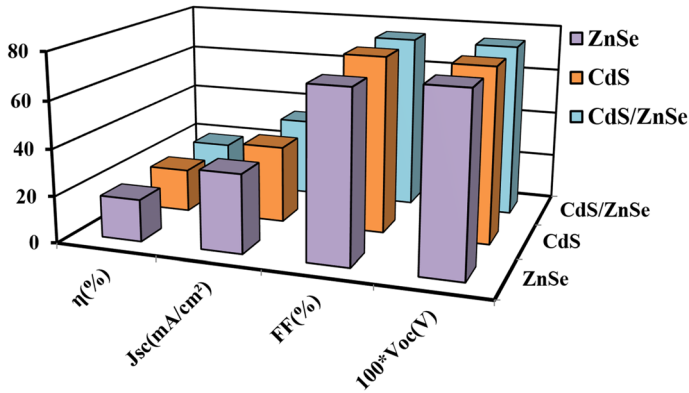


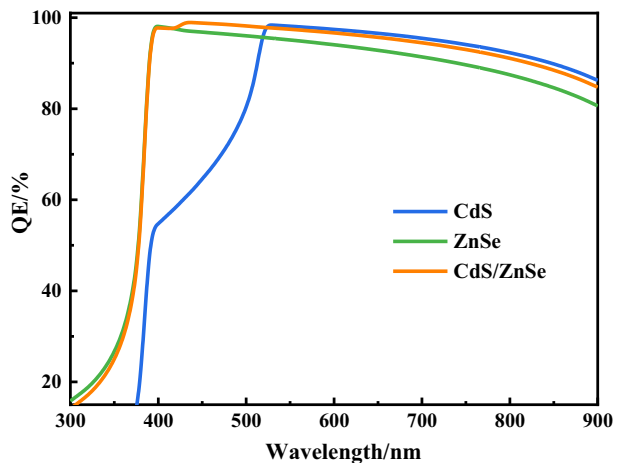
Fig. 9 Photo-current ($J-V$) characteristics simulated for CdS, ZnSe and CdS/ZnSe buffer layers. The V_{OC} values are multiplied by 100

520 nm, the solar cell with CdS/ZnSe double buffer layers have higher response intensity than the other two. In the long wave band, the response of the solar cell with CdS buffer layer is more obvious than that of other solar cells.

Figure 11 shows the energy band of CIGS device with the CdS/ZnSe double buffer layer. The double buffer layer structure has the better performance than ZnSe structure due to the favorable band alignment of the ZnSe/CdS/CIGS interface. In addition, optimization of the thickness of the buffer layer could adjust the depletion region width to realize the better carrier separation.

In order to improve the performance of the CIGS solar cell, the thickness of two different layers of double buffer layer were optimized. The thickness of CdS layer and ZnSe layer increased from 0.01 to 0.05 μm respectively. The simulation results are shown in Fig. 12.

Fig. 10 The QE curve of CIGS cells with CdS, ZnSe and CdS/ZnSe buffer layers



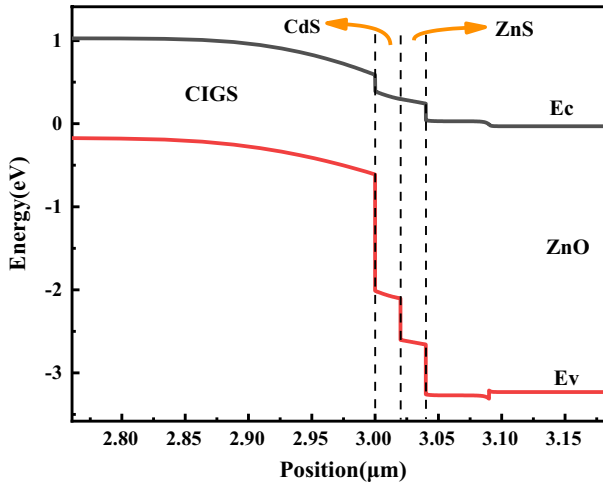


Fig. 11 Energy band diagrammatic sketch of CdS/ZnSe

When both the CdS layer and ZnSe layer are thinner, the V_{oc} and J_{sc} of the solar cell are higher. But thicker CdS and ZnSe layers are not beneficial for FF, as shown in Fig. 12c. For the efficient solar cell, not only high V_{oc} and J_{sc} , but also good FF are required. Therefore, the highest efficiency occurs when the thickness of both layers is close to the middle region, as shown in Fig. 12d. When the thicknesses of CdS and ZnSe layers are $0.03 \mu\text{m}$ and $0.05 \mu\text{m}$, V_{oc} is 0.7446 V, J_{sc} is 33.94 mA/cm^2 , FF is 75.2%, η is 19.01%. The cell efficiency is improved by 9.33% after thickness optimization (Fig. 12d).

4 Conclusions

In this simulation, we used SCAPS software to simulate the performances of CIGS solar cells with different buffer layers (CdS and ZnSe). The results show that the thickness of the buffer layer has a great influence on the main photovoltaic parameters of the solar cell. The thicker buffer layer is beneficial for the V_{oc} and J_{sc} . With increase of thickness of buffer layer, V_{oc} and J_{sc} decrease, but FF increase. For ZnSe buffer layer, the device has better response intensity in short wave band than that with CdS buffer layer, but FF is worse. To further improve the efficiency of the solar cell, we proposed the concept of CdS/ZnSe double buffer layer and found that the optimized double buffer layer has the advantages of CdS and ZnSe materials. The numerical simulations in this paper may be helpful for experimental studies of buffer layers and the improvement of cell performance.

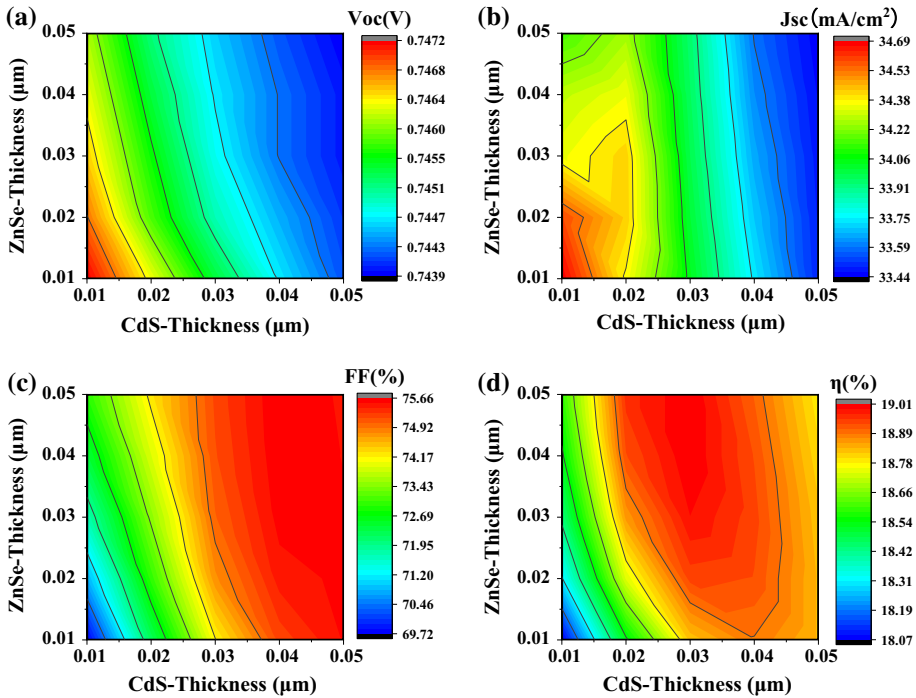


Fig. 12 Effect of buffer thickness of different materials in double buffer layer on cell performance [V_{oc} (a), J_{sc} (b), FF (c), η (d)]

References

- Fischer, J., Larsen, J.K., Guillot, J., Aida, Y., Eisenbarth, T., Regesch, D., Depredurand, V., Fevre, N., Siebenbrunn, S., Dale, P.J.: Composition dependent characterization of copper indium diselenide thin film solar cells synthesized from electrodeposited binary selenide precursor stacks. *Solar Energy Mater. Sol. Cells* **126**, 88–95 (2014)
- Guillemoles, J.F.: The puzzle of Cu(In, Ga)Se₂ (CIGS) solar cells stability. *Thin Solid Films* **403–404**, 405–409 (2002)
- Jackson, P., Hariskos, D., Wuerz, R., Kiowski, O., Bauer, A., Friedlmeier, T.M., Powalla, M.: Properties of Cu(In,Ga)Se₂ solar cells with new record efficiencies up to 21.7%. *Physica Status Solidi (RRL) Rapid Res. Lett.* **9**, 28–31 (2015)
- Kapur, V., Kemmerle, R., Bansal, A., Haber, J., Schmitzberger, J., Le, P., Guevarra, D., Kapur, V., Stempien, T.: Manufacturing of ‘ink based’ CIGS solar cells/modules. In: 2008 33rd IEEE Photovoltaic Specialists Conference (2008)
- Khoshsirat, N., Yunus, N.A.M.: Numerical simulation of CIGS thin film solar cells using SCAPS-1D. In: 2013 IEEE Conference on Sustainable Utilization and Development in Engineering and Technology (CSUDET), p 63 (2013)
- Mostefaoui, M., Mazari, H., Khelifi, S., Bouraiou, A., Dabou, R.: Simulation of high efficiency CIGS solar cells with SCAPS-1D software. *Energy Procedia* **74**, 736–744 (2015)
- Movla, H.: Optimization of the CIGS based thin film solar cells: Numerical simulation and analysis. *Optik* **125**, 67–70 (2014)
- Nakada, T.: Invited paper: CIGS-based thin film solar cells and modules: unique material properties. *Electron. Mater. Lett.* **8**, 179–185 (2012)
- Oyedele, S.O., Aka, B.: Numerical simulation of varied buffer layer of solar cells based on Cigs. *Model. Numer. Simul. Mater. Sci.* **7**, 33–45 (2017)

- Pudov, A.O.: Impact of secondary barriers on copper–indium–gallium–selenide solar-cell operation. ProQuest Dissertations (2005)
- Ramanathan, K., Contreras, M.A., Perkins, C.L., Asher, S., Hasoon, F.S., Keane, J., Young, D., Romero, M., Metzger, W., Noufi, R., Ward, J., Duda, A.: Properties of 19.2% efficiency ZnO/CdS/CuInGaSe₂ thin-film solar cells. *Prog. Photovolt. Res. Appl.* **11**, 225–230 (2003)
- Rampino, S., Armani, N., Bissoli, F., Bronzoni, M., Calestani, D., Calicchio, M., Delmonte, N., Gilioli, E., Gombia, E., Mosca, R., Nasi, L., Pattini, F., Zappettini, A., Mazzer, M.: 15% efficient Cu(In, Ga)Se₂ solar cells obtained by low-temperature pulsed electron deposition. *Appl. Phys. Lett.* **101**(13), 779–894 (2012)
- Reinhard, P., Pianezzi, F., Bissig, B., Chirilă, A., Blösch, P., Nishiwaki, S., Buecheler, S., Tiwari, A.N.: Cu(In, Ga)Se₂ thin-film solar cells and modules—a boost in efficiency due to potassium. *IEEE J. Photovolt.* **5**(2), 656–663 (2015)
- Romeo, A., Terheggen, M., Abou-Ras, D., Bätzner, D., Haug, F.-J., Kaelin, M., Rudmann, D., Tiwari, A.: Development of thin-film Cu(In, Ga)Se₂ and CdTe solar cells. *Prog. Photovolt. Res. Appl.* **12**(2–3), 93–111 (2004)
- Varshni, Y.P.: Temperature dependence of the energy gap in semiconductors. *Physica* **34**, 149–154 (1967)
- Wada, T.: High Efficiency Cu(In,Ga)Se₂ Solar Cells with Improved CIGS surface. In: Proceedings of the 2nd World Conference and Exhibition on Photovoltaic Solar Energy Conversion, 1998, Vienna, Austria (1998)
- Zhang, L., Li, T., Chen, Y., Pang, W., Qu, M., Song, X., Zhang, Y., Yan, H.: Influences of donor defect passivation on the performance of Cu(In, Ga)Se₂ thin-film solar cell. *J. Mater. Sci.: Mater. El.* **29**, 3482–3491 (2018)

Publisher's Note Springer Nature remains neutral with regard to jurisdictional claims in published maps and institutional affiliations.